eLIFE elifesciences.org

SHORT REPORT

Figures and figure supplements

A novel ALS-associated variant in *UBQLN4* regulates motor axon morphogenesis

Brittany M Edens *et al*

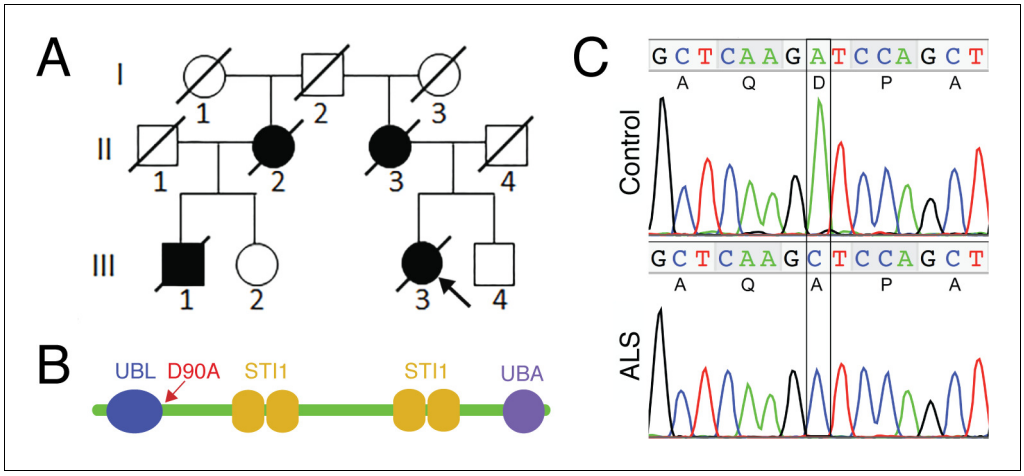

Figure 1. The *UBQLN4* c.269A>C (p.D90A) variant identified in a familial ALS case. (**A**) Pedigree of a family with ALS. The proband (III3, arrow) had disease onset at 55 years of age, with disease duration of 22 months. Her mother (II3) died of ALS at 62 years of age without clear information regarding disease onset. Her maternal grandfather (I2) died in a traffic accident without any known neurological problems. Her maternal aunt (II2) developed ALS with disease onset at 51 years of age, and disease duration of 36 months. Her cousin (III1) developed ALS at 56 years of age and died five years later. (**B**) Predicted structural and functional domains of UBQLN4 with an arrow indicating the position of the mutation site. Domains include a UBL: ubiquitin-like domain, aa 13–83; four STI1 heat-shock-chaperonin-binding motifs, aa 192–229, 230–261, 393–440 and 444–476; and a UBA: ubiquitin-associated domain, aa 558–597. (**C**) Sequencing chromatograms of *UBQLN4* wild-type allele in control and mutant allele in the patient with ALS. An adenine to cytosine substitution is present in the ALS patient, resulting in the change from aspartate to alanine at the ninetieth amino acid, D90A.

DOI: 10.7554/eLife.25453.003

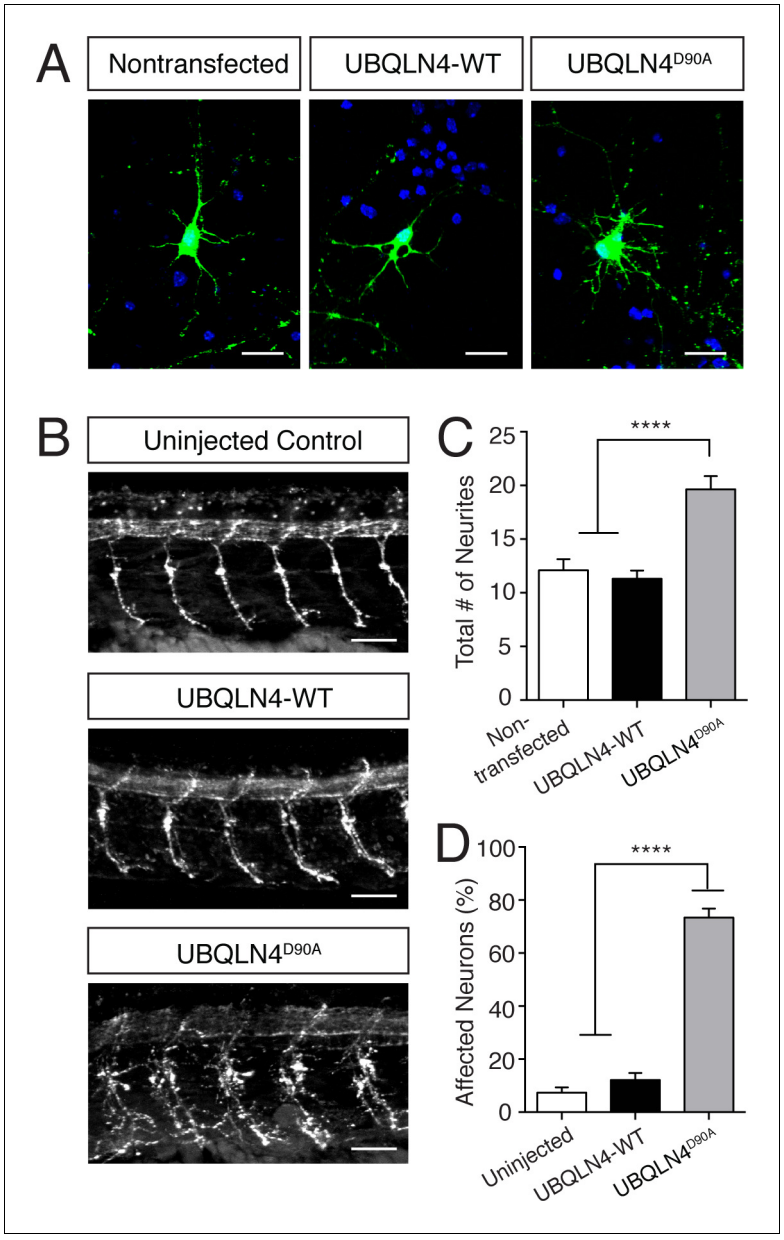

Figure 2. Expression of UBQLN4^{D90A} results in motor axon branching abnormalities in vitro and in vivo. (**A**) Representative images of primary mouse spinal motor neurons transfected with pCAG-GFP alone, or co-transfected with UBQLN4-WT or UBQLN4^{D90A}. Scale bar: 20 µm. (**B**) Representative images of lateral whole-mount zebrafish spinal cords from uninjected, *UBQLN4-WT* mRNA, or *UBQLN4^{D90A}* mRNA injected embryos. Scale bar: 50 µm. (**C**) Quantification of total neurites in (A) revealed an increase in neurite number in UBQLN4^{D90A} transfected neurons compared to pCAG-GFP-only and UBQLN4-WT transfected neurons (n = 30 cells per group, p<0.0001). Data are quantified from three independent experiments and are mean ± SEM. ****p<0.0001, one-way ANOVA with Bonferroni post-hoc test. (**D**) Quantification of percentage of motor axons with aberrant branching in (**B**) revealed an increase in the percentage of affected motor axons in *UBLQN4^{D90A}* injected zebrafish compared to both uninjected and *UBQLN4-WT* injected controls (*n* = 36 embryos per group, p<0.0001). The difference between uninjected and *UBQLN4-WT* injected fish was not significant (p=0.155). The average motor axon length was not significantly different among three groups (p=0.2034). Data are from three independent experiments and are mean ± SEM. ****p<0.0001, one-way ANOVA with Bonferroni post-hoc test.

DOI: 10.7554/eLife.25453.004

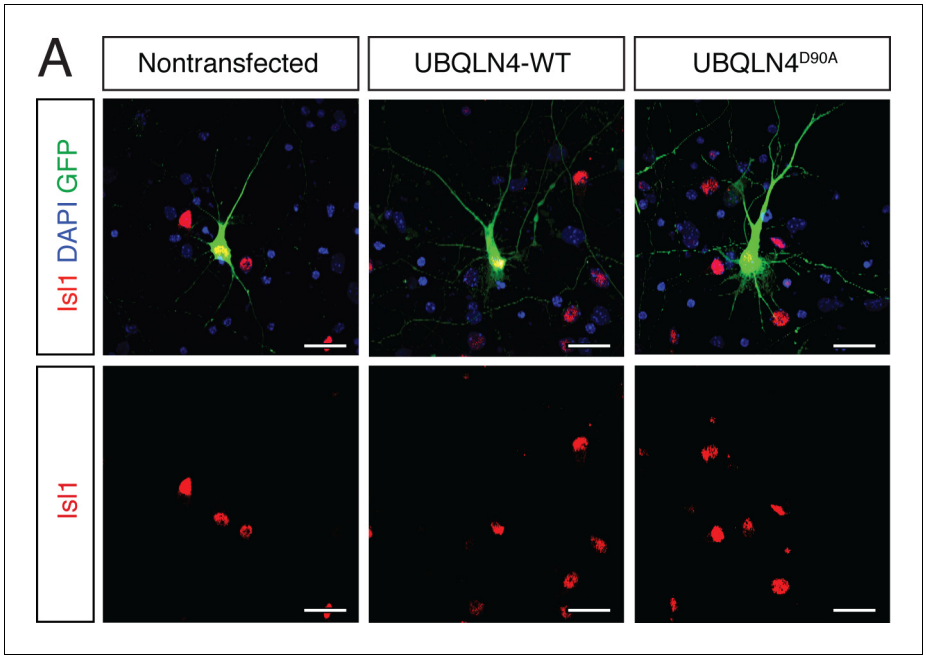

Figure 2—figure supplement 1. Cultured primary motor neurons express the motor neuron marker Islet1. (**A**) Representative images of primary mouse spinal cord neurons transfected with pCAG-GFP and UBQLN4-WT or UBQLN4^{D90A}, stained with Islet1 (red) and DAPI (blue). Scale bar: 20 μm.

DOI: 10.7554/eLife.25453.005

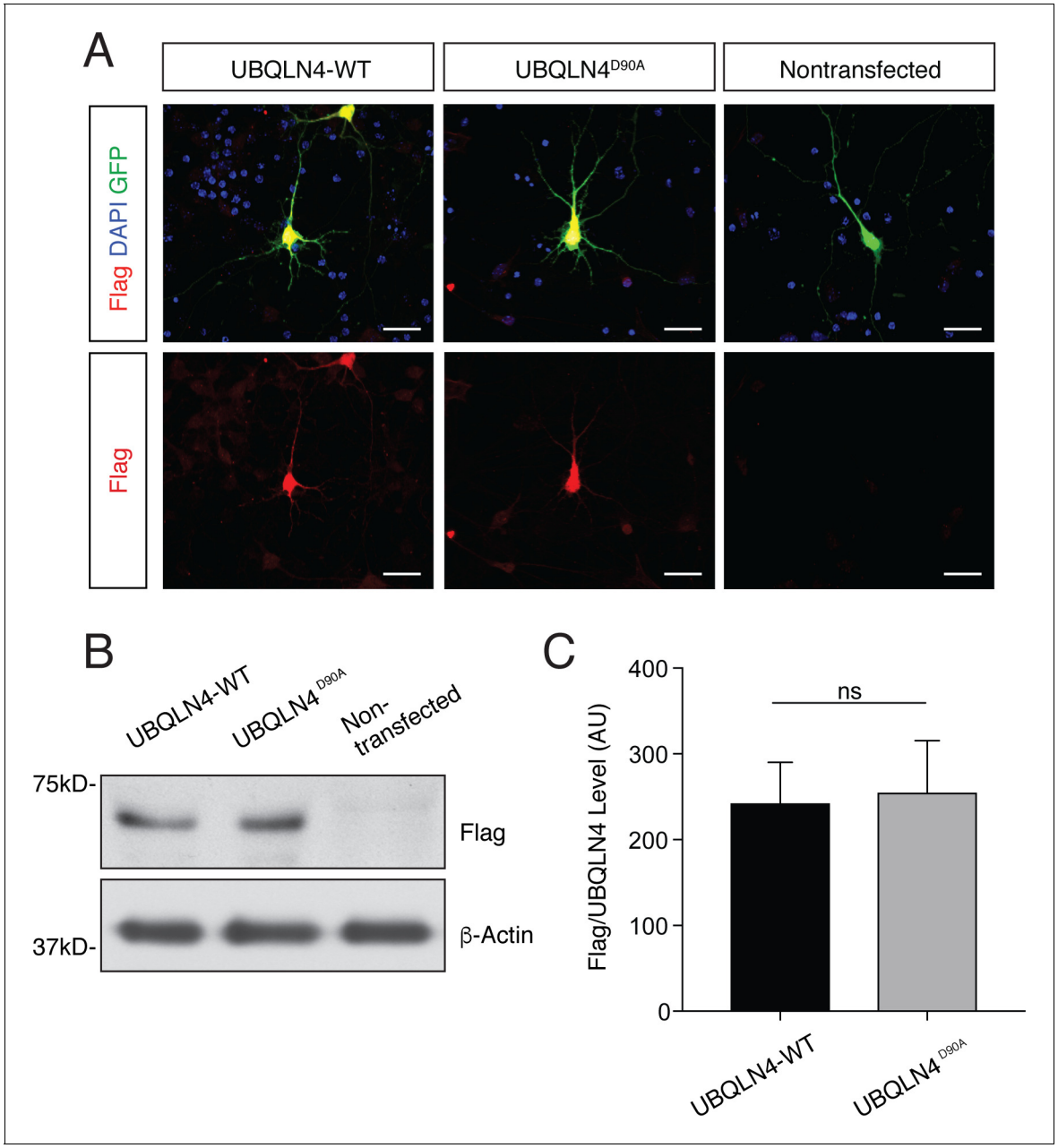

Figure 2—figure supplement 2. UBQLN4-WT and UBQLN4^{D90A} are expressed at similar levels in primary mouse motor neurons and in zebrafish embryos. (**A**) Representative images of primary mouse spinal cord neurons transfected with pCAG-GFP and Flag-tagged UBQLN4-WT or UBQLN4^{D90A}, stained with anti-Flag antibody (red) and DAPI (blue). Scale bar: 20 μm. (**B**) Western blot of UBQLN4/Flag levels from zebrafish embryos injected with *UBQLN4-WT* or *UBQLN4^{D90A}* mRNA, and uninjected controls. Actin Western blot indicates equal protein loading. (**C**) Quantification of Flag signal in (B) confirmed that *UBQLN4-WT* and *UBQLN4^{D90A}* mRNAs are expressed at similar levels (p=0.77). Data are from three independent experiments and are mean ± SEM. ns: p>0.05, two-tailed Student's t-test.

DOI: 10.7554/eLife.25453.006

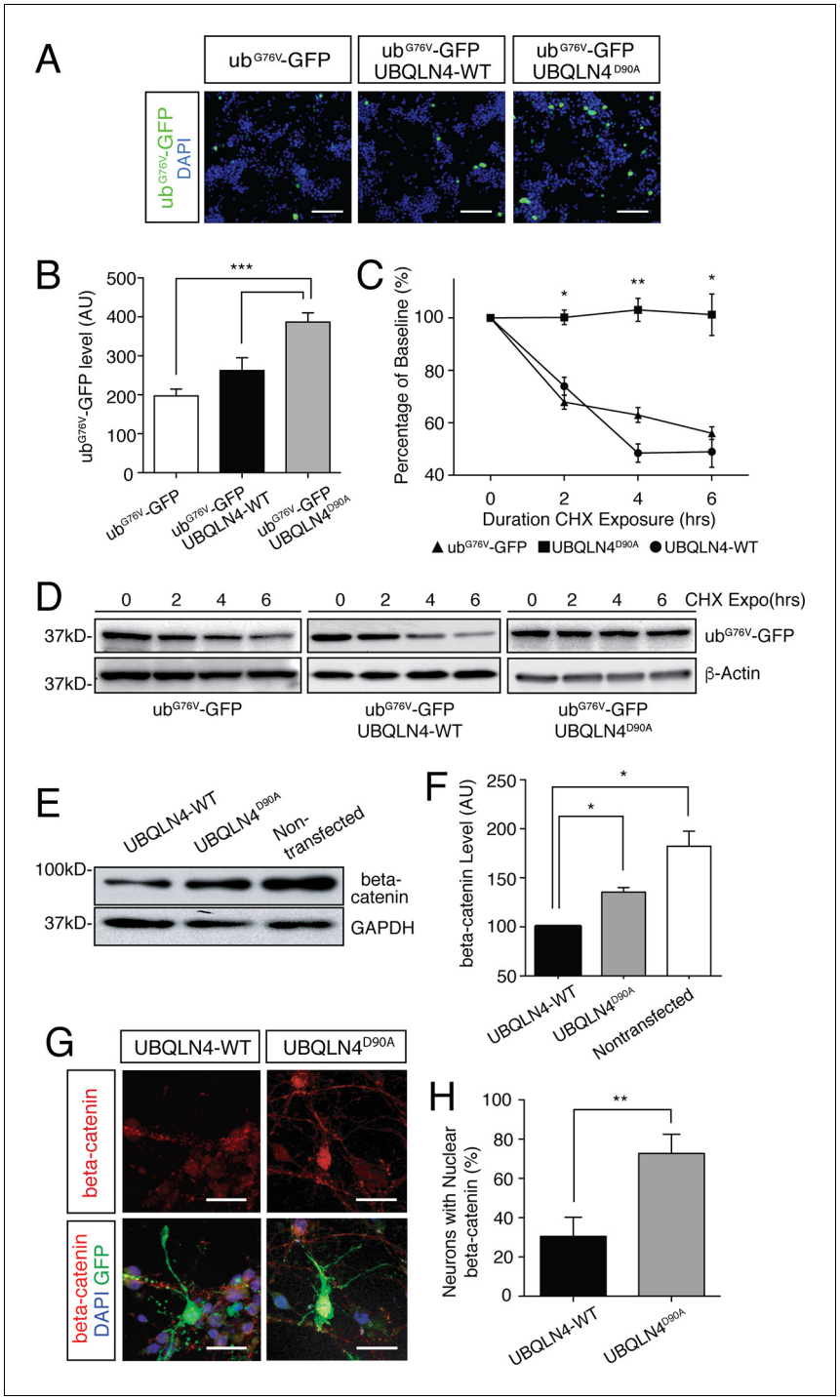

Figure 3. Expression of UBQLN4^{D90A} impairs proteasomal degradation and results in beta-catenin accumulation. (**A**) Representative images of NSC-34 cells transfected with Ub^{G67V}-GFP alone, or co-transfected with UBQLN4-WT or UBQLN4^{D90A}. DAPI staining is shown in blue. Scale bar: 100 µm. (**B**) Quantification of GFP levels in (A) revealed reduced proteasomal turnover following UBQLN4^{D90A} expression. GFP signal, normalized to DAPI, was greater in UBQLN4^{D90A} transfected cells than in Ub^{G67V}-GFP-only transfected cells (p=0.0008), or UBQLN4-WT transfected cells (p=0.0088). The difference in GFP level between Ub^{G67V}-GFP -only and UBQLN4-WT transfected cells was not significant (p=0.1114). Results are from three independent experiments and are mean ± SEM. ***p<0.001, **p<0.01, one-way ANOVA with Bonferroni post-hoc test. (**C**) Cycloheximide protein stability assay. GFP protein stability is compared between Ub^{G67V}-GFP-only, Ub^{G67V}-GFP + UBQLN4-WT, and Ub^{G67V}-GFP + UBQLN4^{D90A} transfected NSC-34 cells treated with cycloheximide for 0, 2, 4, and 6 hr. Quantification of GFP level revealed

Figure 3 continued on next page

Figure 3 continued

impeded protein turnover in UBQLN4^{D90A} transfected cells. GFP level of Ub^{G67V}-GFP + UBQLN4^{D90A} transfected cells was significantly greater than that of Ub^{G67V}-GFP + UBQLN4-WT transfected cells at 2, 4, and 6 hr with cycloheximide treatment (p=0.024 (2 hr), p=0.0038 (4 hr), and p=0.036 (6 hr)). GFP level of Ub^{G67V}-GFP + UBQLN4^{D90A} transfected cells was significantly greater than that of Ub^{G67V}-GFP-only transfected cells (p=0.0068 (2 hr), p=0.0093 (4 hours), and p=0.032 (6 hr)). Results are from three independent experiments and are mean ± SEM. **p<0.01, *p<0.05, one-way ANOVA with Bonferroni post-hoc test. (**D**) Representative Western blot of the cycloheximide protein stability assay. Actin serves as a loading control. (**E**) Western blot of beta-catenin levels from UBQLN4-WT, UBQLN4^{D90A} and non-transfected NSC-34 cells. GAPDH Western blot indicates equal protein loading. (**F**) Quantification of beta-catenin signal in (**D**) indicated greater beta-catenin levels in UBQLN4^{D90A} transfected and non-transfected cells as compared to UBQLN4-WT transfected cells (p=0.0174 and p=0.0326, respectively). Results are from three independent experiments and are mean ± SEM. *p<0.05, one-way ANOVA with Bonferroni post-hoc test. (**G**) Representative images of primary mouse neurons transfected with pCAG-GFP and UBQLN4-WT or UBQLN4^{D90A}, stained for beta-catenin. Scale bar: 20 μm. (**G**) Quantification of beta-catenin localization in (**F**) revealed increased nuclear localization of beta-catenin in UBQLN4^{D90A} transfected cells as compared to UBQLN4-WT transfected cells (*n* = 22 or more cells per group, p=0.0038). Data are from three independent experiments and are mean ± SEM. **p<0.01, two-tailed Student's t-test.

DOI: 10.7554/eLife.25453.007

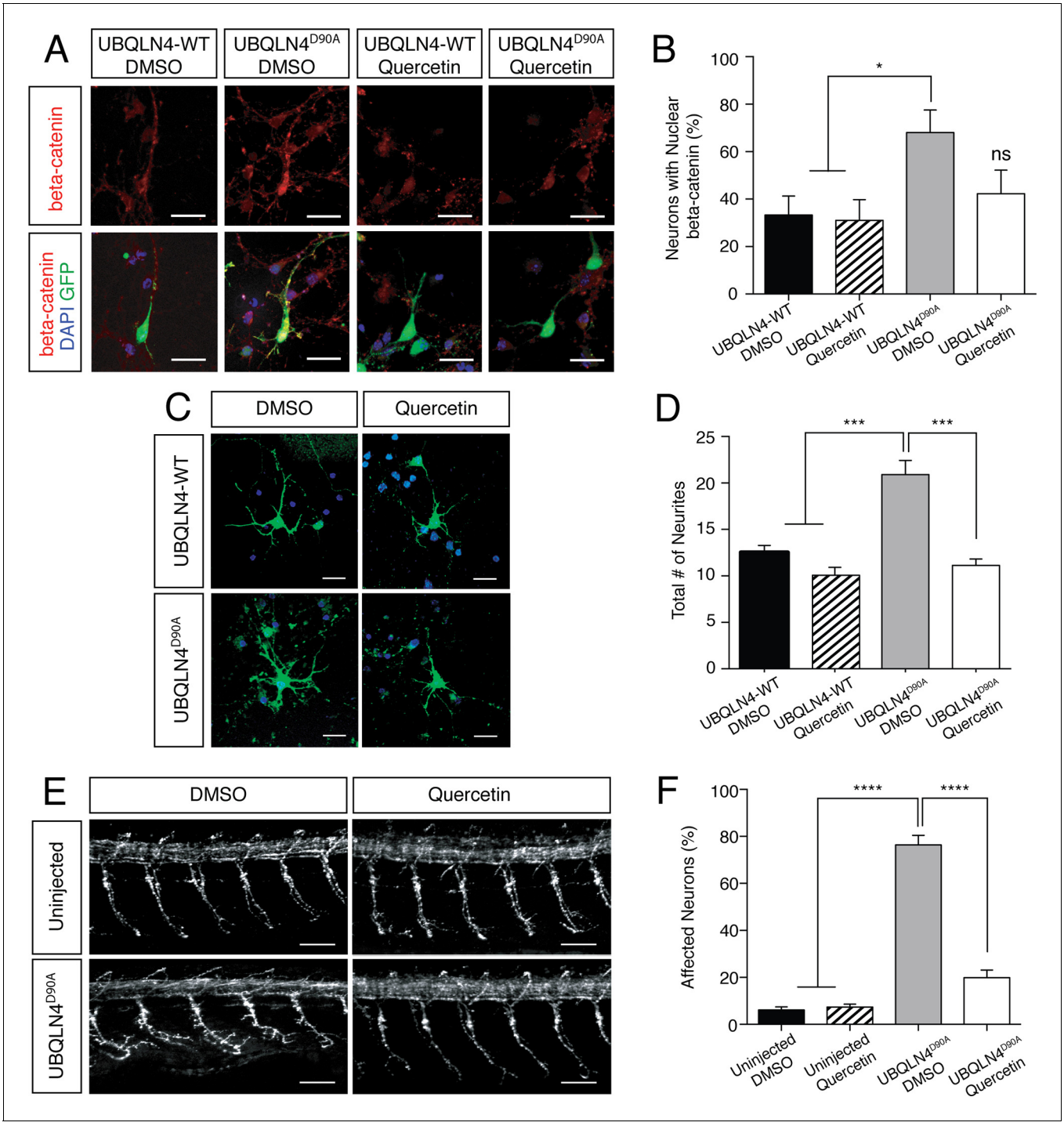

Figure 4. UBQLN4^{D90A}-induced phenotypes are rescued by beta-catenin inhibition. (**A**) Representative images of primary mouse neurons transfected with pCAG-GFP and UBQLN4-WT or UBQLN4^{D90A}, treated with 0.1 µM quercetin or DMSO. Cells are stained for beta-catenin. Scale bar: 20 µm. (**B**) Quantification of beta-catenin localization in (A) revealed a rescue effect of quercetin on increased nuclear localization of beta-catenin caused by UBQLN4^{D90A}. UBQLN4^{D90A} transfected cells showed a dramatic increase of nuclear beta-catenin localization compared to UBQLN4-WT transfected cells (n = 25 or more cells per group, p<0.05). The increase was rescued by the application of quercetin (n = 25 or more cells per group, p=0.48). Data are from three independent experiments and are mean ± SEM. *p<0.05, one-way ANOVA with Bonferroni post-hoc test. (**C**) Representative images of primary mouse spinal cord neurons transfected with pCAG-GFP and UBQLN4-WT or UBQLN4^{D90A}, treated with 0.1 µM quercetin or DMSO. Scale bar: 20 µm. (**D**) Quantification of total neurite numbers in (**C**) revealed a rescue effect of quercetin on increased neurite number in UBQLN4^{D90A} transfected cells. The number of neurites present in UBQLN4^{D90A} transfected cells was significantly greater than that in UBQLN4-WT transfected cells (*n* = 30 cells per group, p<0.0001). Quercetin treatment rescued the increased number of neurites induced by UBQLN4^{D90A} transfection (n = 30 cells per group,

Figure 4 continued on next page

Figure 4 continued

p<0.0001). Data are from three independent experiments and are mean ± SEM. ****p<0.0001, one-way ANOVA with Bonferroni post-hoc test. (**E**) Representative images of lateral whole-mount zebrafish spinal cord from uninjected controls or *UBQLN4*^{D90A} mRNA injected embryos, treated with DMSO or 50 μM quercetin. Scale bar: 50 μm. (**F**) Quantification of the percentage of motor axons with aberrant branching in (**E**) revealed a rescue effect of quercetin on *UBQLN4*^{D90A} injected embryos. *UBQLN4*^{D90A} injected embryos showed a significantly greater percentage of affected motor axons compared to uninjected controls (*n* = 60 embryos per group, p<0.0001). Quercetin treatment rescued aberrant motor axon branching in *UBQLN4*^{D90A} injected embryos (*n* = 60 embryos per group, p<0.0001). Data are from three independent experiments and are mean ± SEM. ****p<0.0001, one-way ANOVA with Bonferroni post-hoc test.

DOI: 10.7554/eLife.25453.008

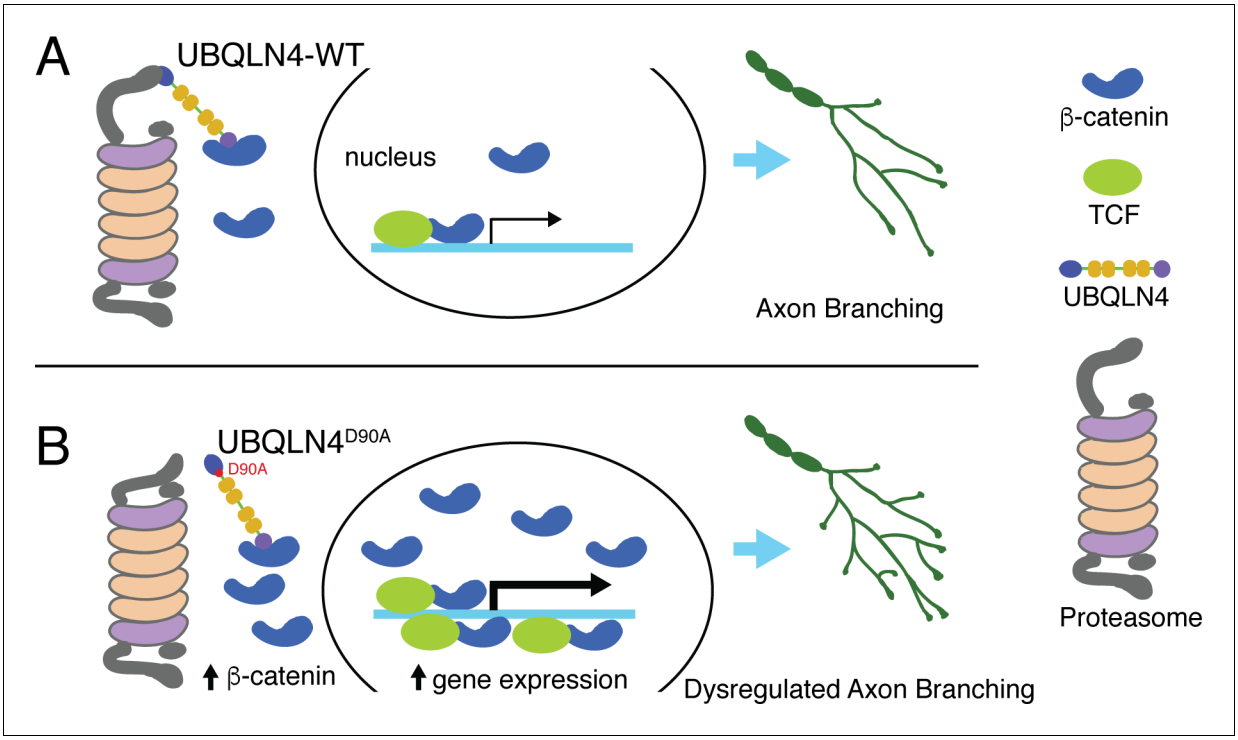

Figure 5. Schematic model illustrating proposed roles for wild-type (A) and ALS-associated *UBQLN4*^{D90A} (B) in motor axon morphogenesis. (**A**) Wild-type *UBQLN4* associates with beta-catenin through its UBA domain, and with the proteasome through its UBL domain. These interactions allow for the degradation of beta-catenin, which in turn modulates gene expression to control motor axon morphogenesis. (**B**) The ALS-associated *UBQLN4*^{D90A} variant is deficient in mediating proteasomal degradation of beta-catenin, leading to its accumulation and excessive induction of gene expression. Hyperactivation of beta-catenin-controlled genes dysregulates axon morphogenesis, causing aberrant axon branching in motor neurons.
DOI: 10.7554/eLife.25453.009